States of fermionic atoms in an optical superlattice across a Feshbach resonance

T. Goodman and L.-M. Duan
FOCUS center and MCTP, Department of Physics, University of Michigan, Ann Arbor, MI 48109

We investigate states of fermionic atoms across a broad Feshbach resonance in an optical superlattice which allows interaction only among a small number of lattice sites. The states are in general described by superpositions of atomic resonating valence bonds and dressed molecules. As one scans the magnetic field, level crossing is found between states with different symmetry properties, which may correspond to a quantum phase transition in the many-body case.

PACS numbers: 34.10.+x, 03.75.Ss, 05.30.Fk, 34.50.-s

I. INTRODUCTION

The past several years have seen many new developments in ultracold atomic physics [1, 2]. Two experimental control techniques have played a critical role in these advances: the use of optical lattices to produce diverse interaction configurations [3], and Feshbach resonance to control the strength of the interactions between atoms [4]. This has motivated significant interest in combining these two techniques [5, 6, 7, 8, 9, 10].

Close to a broad Feshbach resonance, one then has strongly interacting fermions in a lattice, with the effective interaction energy easily larger than the band gap. For such a strongly correlated system, in general it is very hard to understand its physics. As the first step, one may try to understand the single-site physics, which contains the dominant interactions for the atoms in a deep optical lattice. The two-body physics on a single site has been solved exactly in [8] under typical experimental configurations, and it is found there that many bands of the lattice are significantly populated, in agreement with the experimental observation [9]. In the next step, it is natural to consider interactions over a few lattice sites. We have shown in [6] that for the case of a multiple-site lattice, one needs to take into account the direct collision interactions between the neighboring sites, as the magnitude of this interaction is larger than the atom tunneling rate for a typical wide Feshbach resonance such as with ^{40}K or ^{6}Li atoms. An effective lattice interaction Hamiltonian has been derived there, which takes into account both the multi-band populations and the direct off-site and on-site collisions. In this effective Hamiltonian, whenever two atoms come to the same lattice site, they form a dressed molecule state (a single-site Cooper pair), which corresponds to an exact eigenstate constructed from the single-site physics. The effective Hamiltonian then describes the interaction between these dressed molecules and the atoms over different lattice sites. The explicit form of the Hamiltonian is as follows [6]

$$\begin{aligned} H_{eff} &= \sum_i \Delta(B) d_i^\dagger d_i + \sum_{i;j\in N(i)} t_d P d_i^\dagger d_j P \\ &+ \sum_{i;j\in N(i)} \sum_\sigma \left(t_a P a_{i\sigma}^\dagger a_{j\sigma} P + t_{da} d_i^\dagger d_j a_{j\sigma}^\dagger a_{i\sigma} \right) \\ &+ \sum_{i;j\in N(i)} \left(g d_i^\dagger \left(a_{i\uparrow} a_{j\downarrow} - a_{i\downarrow} a_{j\uparrow} \right) + h.c. \right) \end{aligned} \quad (1)$$

where $a^\dagger$ and $d^\dagger$ represent creation operators for fermionic atoms and bosonic dressed molecules, respectively; $\sigma = \uparrow, \downarrow$ labels two internal spin states; and i labels the lattice sites (with $j \in N(i)$ labeling the sites adjacent to i). P represents a projection of the state at every lattice site i onto the four-dimensional subspace with basis $\left\{ |0\rangle_i, a_{i\uparrow}^\dagger |0\rangle_i, a_{i\downarrow}^\dagger |0\rangle_i, d_i^\dagger |0\rangle_i \right\}$. The parameters g, t_d, t_a, and t_{da} depend on the physical properties of the atomic system as well as the multi-band properties of the optical lattice (see the explicit expressions in [6]). The parameter Δ corresponds to an eigenenergy of the two-body physics from a single site, and can be tuned over a wide range of values by varying the applied magnetic field B [8].

In this paper, we make use of the above effective Hamiltonian H_{eff} to study the physics of this strongly correlated system with interactions among a few lattice sites. In particular, we focus on investigation of the states of a single plaquette, which is a basic unit of the two-dimensional square lattice. This study has two purposes. First, understanding the states of atoms at a single plaquette is a necessary step towards the challenging goal of understanding the physics of this strongly interacting gas in a quasi-two-dimensional optical lattice. It is shown in [6] that the effective Hamiltonian H_{eff} reduces to the well-known t-J model [11] and the XXZ model [12] in certain limits of the parameter values, so the physics associated with H_{eff} should be rich and parameter-dependent. In this work, we would like to understand the influence of the parameters on a few body physics, and that understanding will provide an intuition for taking appropriate approximations towards the many-body physics. In particular, from the few-body physics, we construct states which will provide the basic entries for an effective many-body theory through the contractor renormalization procedure (a real-space renormalizaton group method for high dimensions) [13, 14]. We will see that even for a single plaquette, the behavior of the states has been pretty rich. The eigenstates involve resonating valence bonds and superposition of dressed molecules, and are highly entangled over different lattice sites. With variation of the parameters in the Hamiltonian H_{eff}, there are sev-

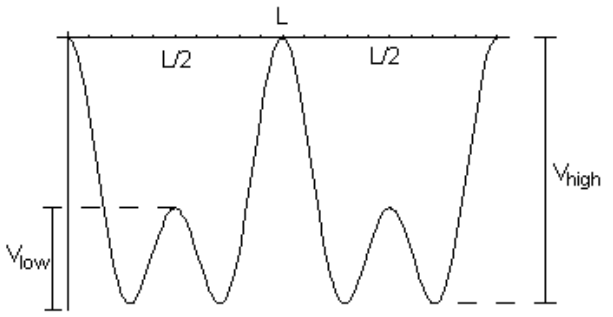

FIG. 1: Superlattice potential vs. x for $V(x) = -\left(V_1 sin^2\left(\frac{\pi x}{L}\right) + V_2 sin^2\left(\frac{2\pi x}{L}\right)\right)$

eral level crossings for the lowest eigenstate with change of the state symmetry properties, which may correspond to a quantum phase transition for larger systems.

Second, the study of the physics of a single plaquette is also of practical relevance. For atoms in an optical superlattice, the physics can be dominated by the interactions within single plaquettes. A simple optical superlattice can be formed by adding two standing wave laser beams with commensurate wave vectors [15, 16]. The potential, say, along the x direction, has the form $V(x) = -\left[V_1 sin^2(k_1 x) + V_2 sin^2(k_2 x)\right]$. If we choose the wave vector $k_2 = 2k_1 = 2\pi/L$ and require $0 < V_1 < 4V_2$, then we have potential barriers of two different heights (see FIG. 1). The minima occur at $x = nL \pm x_0$ (for integer n), where

$$x_0 = \frac{L}{2\pi} cos^{-1}\left(\frac{-V_1}{4V_2}\right) \tag{2}$$

The lower and higher potential barriers V_{low} and V_{high} are given respectively by

$$\begin{aligned} V_{low} &= \left(1 - \frac{V_1}{4V_2}\right)^2 V_2 \\ V_{high} &= \left(1 + \frac{V_1}{4V_2}\right)^2 V_2. \end{aligned} \tag{3}$$

The barrier V_{high} can be significantly larger than V_{low} if we choose V_1 close to $4V_2$, and such a high barrier turns off the interactions except for the ones between the sites separated by V_{low}. If we apply this optical superlattice potential along both the x and y directions and a deep lattice potential along the z direction, we then have interactions dominantly within the single plaquettes in the x-y plane. With strongly interacting atoms in this optical superlattice potential, one can test the predictions from the effective Hamiltonian H_{eff}, and detect the exotic entangled states emerging from the ground state configurations of H_{eff}.

We should also point out that the effective Hamiltonian H_{eff} includes the Hubbard model as a particular case. The Hubbard model is given by the Hamiltonian [14, 17]

$$H_{Hub} = -t \sum_{<i,j>,\sigma} \left(a^\dagger_{i\sigma} a_{j\sigma} + H.c.\right) + U \sum_i n_{i\uparrow} n_{i\downarrow}, \tag{4}$$

where $n_{i\sigma} = a^\dagger_{i\sigma} a_{i\sigma}$. Specifically, H_{eff} can be written in the form of H_{Hub} if we substitute $d^\dagger_i$ with $a^\dagger_{i\uparrow} a^\dagger_{i\downarrow}$ and make a particular choice of the parameters in H_{eff} with $t_a = -t$, $t_{da} = t$, $g = t$, $t_d = 0$, and $\Delta = U$. So, one can see that H_{eff} extends the well-known Hubbard model H_{Hub} in a nontrivial way. Note that for strongly interacting atoms near a broad Feshbach resonance, the parameters g and t_{da} are significantly different from the atomic tunneling rate t due to the multi-band populations and the direct neighboring collisions. From the expressions of these parameters in Ref. [6], we estimate that typically $|t_d| << |t_a| << |t_{da}| \sim |g|$. This is because t_a corresponds to atomic tunneling in the single lowest band, whereas t_{da} and g correspond to interactions involving the dressed molecule states (which are superpositions of states in multiple upper bands). For the numerical calculations in this work, we typically take $t_d \sim 0$, $-t_a \sim 0.1|g|$–$0.3|g|$, and $t_{da} \sim |g|$–$2|g|$. (Note from the form of H_{eff} that the sign of g is essentially irrelevant, as it can be incorporated into the definition of $d^\dagger$.) The parameter Δ is sensitive to the external magnetic field, and can be scanned from the value much smaller than $-|g|$ to the value much larger than $|g|$.

The atomic states within each plaquette critically depend on the atom number and the spin configuration in that plaquette. In the following, we will consider all the different nontrivial cases with different numbers of spin $\uparrow$ and $\downarrow$ atoms occupying the four-site plaquette.

II. FOUR ATOMS PER PLAQUETTE: TWO $\uparrow$, TWO $\downarrow$

Over most of the typical range of the parameter values, the plaquette occupied by two $\uparrow$ and two $\downarrow$ atoms has two distinct types of ground states, with a level crossing occurring at some critical value of Δ. These two types of states can be distinguished by how they transform under a 90° rotation in the plane of the plaquette. Under such a rotation, the ground state wavefunction for Δ less than (greater than) the critical value is multiplied by a factor of $+1$ (-1). Thus, we say that the phase on the negative side of the transition has s-wave symmetry, and that on the positive side has d-wave symmetry.

The ground states of each of these two types change smoothly with changes in the parameter Δ. Thus, we can identify particular energy eigenstates as the "s-wave state" and the "d-wave state" over the full range of Δ, even as the exact form of the eigenstate changes. (Note that these are not the *only* eigenstates with s-wave and d-wave symmetry – here we use these terms to refer solely to those states which are the ground states when the system is in the corresponding parameter regions.) The

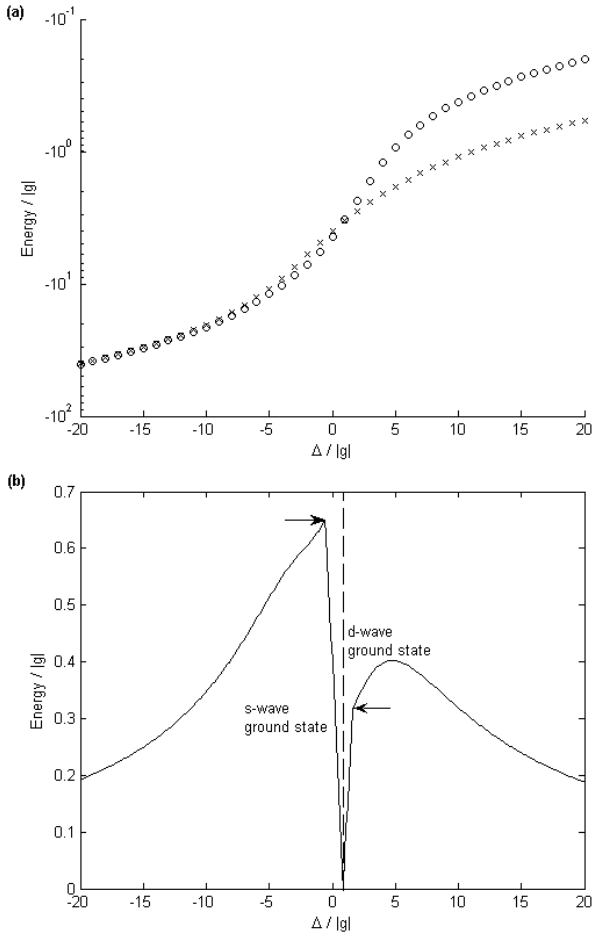

FIG. 2: Energy vs. Δ for a plaquette occupied by two $\uparrow$ and two $\downarrow$ atoms. Other parameters are $t_{da} = 1.5|g|$, $t_a = -0.2|g|$, $t_d = 0$ (a): Eigenenergies of the s-wave ($\circ$) and d-wave (x) states. (b): Energy difference (gap) between ground state and first excited state. The gap vanishes at the level crossing point. Because the eigenenergies vary smoothly with Δ, the curve is smooth except at the level crossing points for the ground state (where the gap is zero) and for the first excited state (indicated by arrows)

energies of the s-wave and d-wave states can be easily calculated through exact diagonalization, and they are plotted in FIG. 2(a), which illustrates the crossover between them. (For this figure, we scan Δ and set the other parameters of H_{eff} to their typical values with $t_{da} = 1.5|g|$ and $t_a = -0.2|g|$.) The energy gap between the ground state and 1st excited state is shown in FIG. 2(b)).

To understand the properties of the ground state, it is important to have its explicit expression. Although one can calculate this explicit expression through numerical exact diagonalization, the state is in general a superposition of many basis-vectors (36 vectors in this case), with all the superposition coefficients varying with Δ. It is troublesome to understand the state's properties from this lengthy expression. To overcome this problem, we describe the s-wave and d-wave states more compactly, in a way that illustrates their rotational symmetry, by means of a pictorial representation which we define here. The four sites of a plaquette we label as: $\begin{smallmatrix}1 & 2\\ 3 & 4\end{smallmatrix}$. We place various pictures on these sites corresponding to creation operators applied at those sites. The whole picture represents the product of these operators, applied to the vacuum state $|0\rangle$. For instance, $\begin{smallmatrix}\bullet\\ \bullet\end{smallmatrix}$ placed on two sites (either horizontally, vertically, or diagonally) represents a normalized singlet between those two sites. So, if the sites are labeled i and j, this represents $\frac{1}{\sqrt{2}}\left(a^\dagger_{i\uparrow}a^\dagger_{j\downarrow} - a^\dagger_{i\downarrow}a^\dagger_{j\uparrow}\right)$. (Note that the order of i and j does not matter, as the anti-commutation of $a^\dagger_i$ and $a^\dagger_j$ makes the singlet symmetric under exchange of i and j.) $\textcircled{m}$ represents a dressed molecule. (I.e., if located at site i , this picture corresponds to $d^\dagger_i$.) $\circ$ represents an unoccupied site. The creation operators that make up a singlet are always grouped together; other than that, the order of the operators is irrelevant, as the singlets and dressed molecules commute. As an example, the picture $\begin{smallmatrix}\bullet & \textcircled{m}\\ \bullet & \circ\end{smallmatrix}$ represents $\frac{1}{\sqrt{2}}\left(a^\dagger_{1\uparrow}a^\dagger_{3\downarrow} - a^\dagger_{1\downarrow}a^\dagger_{3\uparrow}\right) d^\dagger_2 |0\rangle$.

The full Hilbert space for two $\uparrow$ and two $\downarrow$ atoms on a plaquette is 36-dimensional. However, the s-wave state (over the full range of Δ) can be conveniently expressed as a vector in a 4-dimensional subspace of the full space, with basis vectors:

$$|1\rangle_s = \frac{1}{2\sqrt{3}}\left[\begin{smallmatrix}\textcircled{m} & \textcircled{m}\\ \circ & \circ\end{smallmatrix} + \begin{smallmatrix}\circ & \textcircled{m}\\ \circ & \textcircled{m}\end{smallmatrix} + \begin{smallmatrix}\circ & \circ\\ \textcircled{m} & \textcircled{m}\end{smallmatrix} + \begin{smallmatrix}\textcircled{m} & \circ\\ \textcircled{m} & \circ\end{smallmatrix} + 2\left(\begin{smallmatrix}\textcircled{m} & \circ\\ \circ & \textcircled{m}\end{smallmatrix} + \begin{smallmatrix}\circ & \textcircled{m}\\ \textcircled{m} & \circ\end{smallmatrix}\right)\right]$$

$$|2\rangle_s = \frac{1}{2\sqrt{2}}\left(\begin{smallmatrix}\bullet & \textcircled{m}\\ \circ & \end{smallmatrix} + \begin{smallmatrix}\bullet & \bullet\\ \circ & \textcircled{m}\end{smallmatrix} + \begin{smallmatrix}\circ & \bullet\\ \textcircled{m} & \end{smallmatrix} + \begin{smallmatrix}\textcircled{m} & \circ\\ \bullet & \bullet\end{smallmatrix} + \begin{smallmatrix}\bullet & \circ\\ \textcircled{m} & \end{smallmatrix} + \begin{smallmatrix}\bullet & \bullet\\ \textcircled{m} & \circ\end{smallmatrix} + \begin{smallmatrix}\circ & \textcircled{m}\\ \bullet & \bullet\end{smallmatrix}\right)$$

$$|3\rangle_s = \frac{1}{2}\left(\begin{smallmatrix}\textcircled{m} & \\ & \circ\end{smallmatrix} + \begin{smallmatrix} & \textcircled{m}\\ \circ & \end{smallmatrix} + \begin{smallmatrix}\circ & \\ & \textcircled{m}\end{smallmatrix} + \begin{smallmatrix} & \circ\\ \textcircled{m} & \end{smallmatrix}\right)$$

$$|4\rangle_s = \begin{smallmatrix}\bullet & \bullet\\ \bullet & \bullet\end{smallmatrix} + \begin{smallmatrix}\bullet & \\ \bullet & \end{smallmatrix}\begin{smallmatrix} & \bullet\\ & \bullet\end{smallmatrix}$$

The d-wave state (as Δ varies) can be written as a vector in a 3-dimensional subspace with basis vectors:

$$|1\rangle_d = \frac{1}{2}\left(\begin{smallmatrix}\textcircled{m} & \textcircled{m}\\ \circ & \circ\end{smallmatrix} - \begin{smallmatrix}\circ & \textcircled{m}\\ \circ & \textcircled{m}\end{smallmatrix} + \begin{smallmatrix}\circ & \circ\\ \textcircled{m} & \textcircled{m}\end{smallmatrix} - \begin{smallmatrix}\textcircled{m} & \circ\\ \textcircled{m} & \circ\end{smallmatrix}\right)$$

$$|2\rangle_d = \frac{1}{2\sqrt{2}}\left(\begin{smallmatrix}\textcircled{m} & \bullet\\ \circ & \end{smallmatrix} - \begin{smallmatrix}\circ & \textcircled{m}\\ \bullet & \end{smallmatrix} + \begin{smallmatrix}\bullet & \circ\\ \textcircled{m} & \end{smallmatrix} - \begin{smallmatrix}\bullet & \\ \textcircled{m} & \circ\end{smallmatrix} + \begin{smallmatrix}\circ & \bullet\\ \textcircled{m} & \end{smallmatrix} - \begin{smallmatrix}\textcircled{m} & \circ\\ \bullet & \end{smallmatrix} + \begin{smallmatrix}\bullet & \textcircled{m}\\ \circ & \end{smallmatrix} - \begin{smallmatrix}\bullet & \bullet\\ \circ & \textcircled{m}\end{smallmatrix}\right)$$

$$|3\rangle_d = \frac{1}{\sqrt{3}}\left(\begin{smallmatrix}\bullet & \bullet\\ \bullet & \end{smallmatrix} - \begin{smallmatrix}\bullet & \bullet\\ \bullet & \end{smallmatrix}\right)$$

Note that $|4\rangle_s$ and $|3\rangle_d$ are written here as sums of *non-orthogonal* terms; however, this form makes their rotational symmetry readily apparent. The states $|4\rangle_s$ and $|3\rangle_d$ are the resonating valence bond (RVB) states for atoms on a single plaquette [11, 14], with s and d wave symmetries, respectively. For a larger lattice, the RVB states are in general superpositions of many different spin-singlet distribution patterns [18].

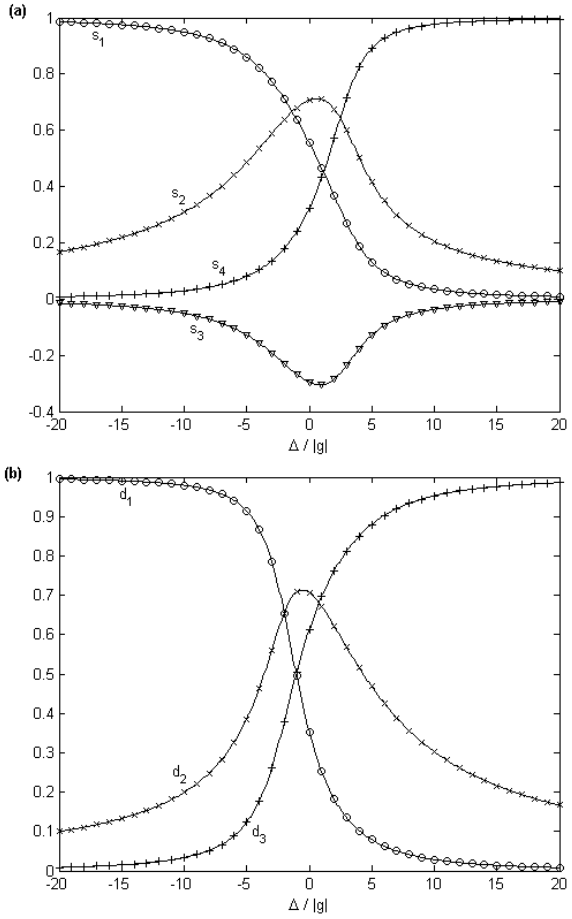

FIG. 3: The ground-state configuration vs. the detuning Δ for a plaquette occupied by two $\uparrow$ and two $\downarrow$ atoms. ($t_{da} = 1.5|g|$, $t_a = -0.2|g|$, $t_d = 0$) (a) Components of the s-wave state (s_1: $\circ$, s_2: x, s_3: $\bigtriangledown$, s_4 : +). (b) Components of the d-wave state (d_1: $\circ$, d_2: x, d_3: +). The marked data points were computed from the full Hamiltonian H_{eff}, whereas the solid lines were computed from the projected Hamiltonians H_s and H_d, respectively.

Thus the s-wave and d-wave ground states, respectively, are:

$$|\psi\rangle_s = s_1 |1\rangle_s + s_2 |2\rangle_s + s_3 |3\rangle_s + s_4 |4\rangle_s , \quad (5)$$

$$|\psi\rangle_d = d_1 |1\rangle_d + d_2 |2\rangle_d + d_3 |3\rangle_d , \quad (6)$$

They are superpositions of many different distribution patterns of the dressed molecules and the atomic valence bonds (spin singlets). The values of the superposition coefficients are shown in FIG. 3 as a function of the ratio $\Delta/|g|$. Note that in the limiting case $\Delta/|g| >> 1$, the effective Hamiltonian H_{eff} reduces to the t-J model [6]. Indeed, one can see from FIG. 3 that the state $|\psi\rangle_d$ in that limit tends to the ground state $|3\rangle_d$ of the t-J model on a plaquette [11].

Projected onto these subspaces, H_{eff} (with $t_d \simeq 0$) expressed in terms of the bases shown above becomes:

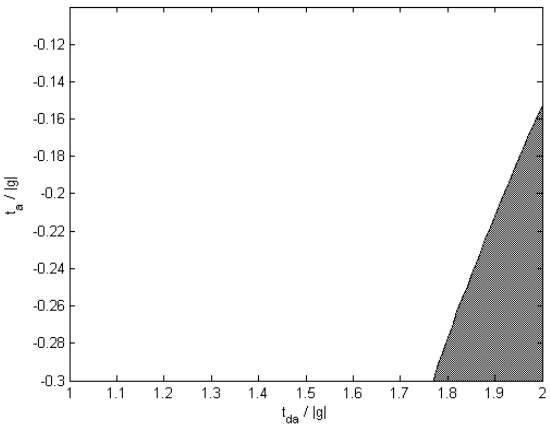

FIG. 4: In the typical range of $t_{da}/|g|$ and $t_a/|g|$, the s-wave triplet ground state of the plaquette with 2 $\uparrow$ and 2 $\downarrow$ atoms occurs for parameter values within the shaded region.

$$H_s = \begin{pmatrix} 2\Delta & -2\sqrt{3}g & 0 & 0 \\ -2\sqrt{3}g & \Delta & \sqrt{2}\,(t_a + t_{da}) & -2g \\ 0 & \sqrt{2}\,(t_a + t_{da}) & \Delta & 0 \\ 0 & -2g & 0 & 0 \end{pmatrix} \quad (7)$$

for the s-wave state, and:

$$H_d = \begin{pmatrix} 2\Delta & -2g & 0 \\ -2g & \Delta & -2\sqrt{3}g \\ 0 & -2\sqrt{3}g & 0 \end{pmatrix} \quad (8)$$

for the d-wave state. The lowest energy eigenstates of these two Hamiltonians are the s-wave and d-wave states (respectively) of the full Hamiltonian H_{eff}. (See solid lines on FIG. 3.)

For a small portion of the range of the parameter values $t_{da}/|g|$ and $t_a/|g|$ there is an additional type of ground state, which occurs for Δ between the s-wave and d-wave states above. For this type, the ground state also has s-wave rotational symmetry. However, the states $\uparrow$ and $\downarrow$ are in a triplet configuration, rather than the singlet occurring in the other two types of states $|\psi\rangle_s$ and $|\psi\rangle_d$. The region of the parameter space for which this triplet phase occurs is shown in FIG. 4. The eigenenergies of the s-wave singlet, s-wave triplet, and d-wave singlet states are shown in FIG. 5(a) for $t_{da} = 2|g|$, $t_a = -0.3|g|$ (which is within the range where the triplet ground state occurs.) The gap between the ground state and first excited state for $t_{da} = 2|g|$, $t_a = -0.3|g|$ is shown in FIG. 5(b).

The s-wave triplet state can be written as a linear combination of three states:

$|1\rangle_{trip} = \frac{1}{2\sqrt{2}}$ (

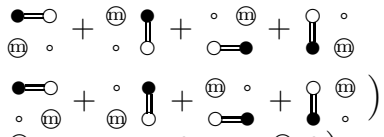

)

$|2\rangle_{trip} = \frac{1}{2}$ (

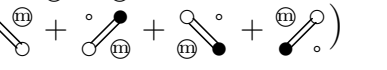

)

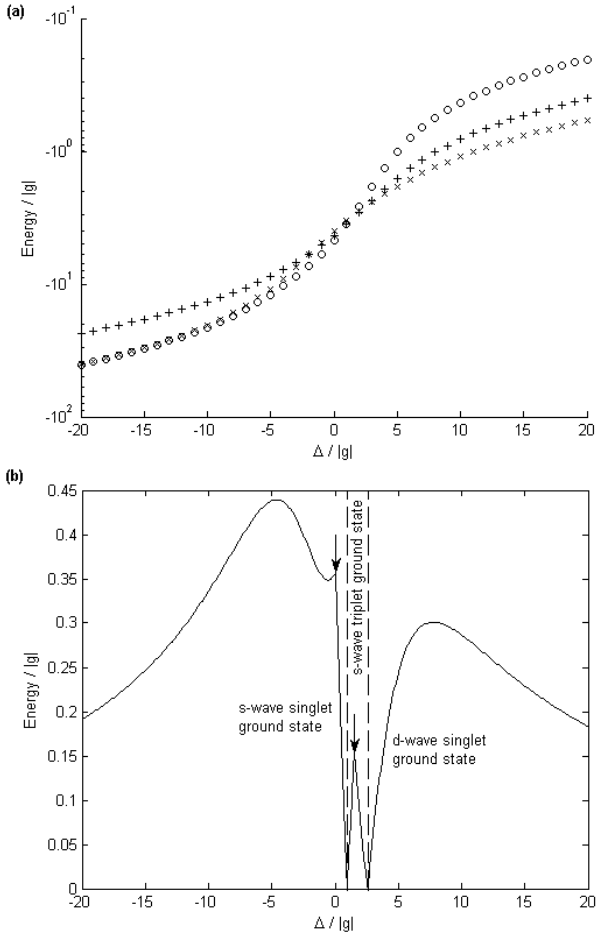

FIG. 5: Energy vs. Δ for a plaquette occupied by two $\uparrow$ and two $\downarrow$ atoms. Other parameters are $t_{da} = 2|g|$, $t_a = -0.3|g|$, $t_d = 0$ (a): Eigenenergies of the s-wave singlet ($\circ$), d-wave singlet (x), and s-wave triplet (+) states. (b): Energy difference between ground state and first excited state. Crossovers in the first excited state are indicated by arrows.

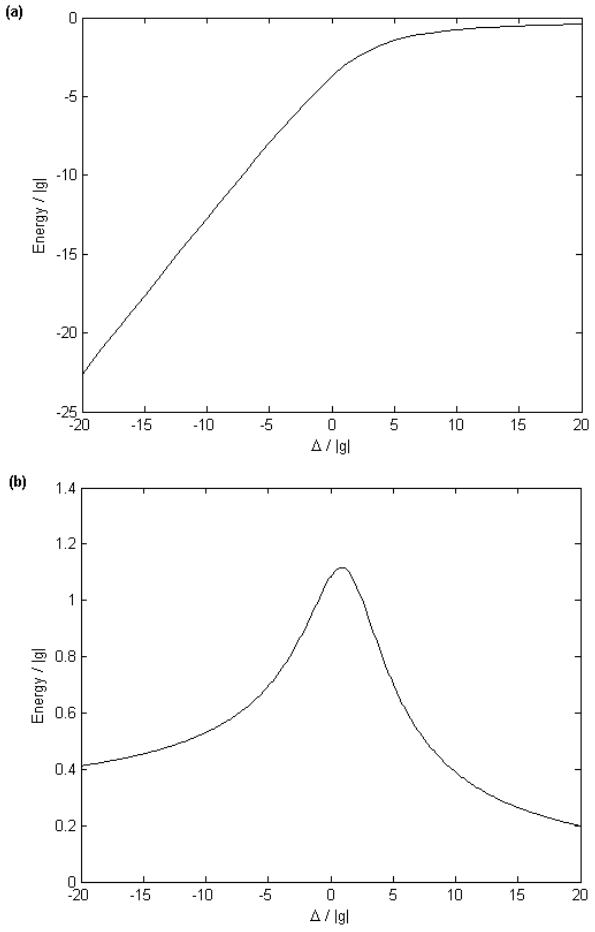

FIG. 6: Energy vs. Δ for a plaquette occupied by three $\uparrow$ and one $\downarrow$ atoms. Other parameters are $t_{da} = 1.5|g|$, $t_a = -0.2|g|$, $t_d = 0$ (a): Ground state energy. (b): Energy difference between ground state and first excited state.

$$|3\rangle_{trip} = \frac{1}{2\sqrt{2}}\Big($$ 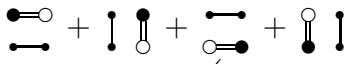 $$\Big)$$

Here  represents the triplet $\frac{1}{\sqrt{2}}\left(a^\dagger_{i\uparrow}a^\dagger_{j\downarrow} + a^\dagger_{i\downarrow}a^\dagger_{j\uparrow}\right)$, where i is the site of the black-filled circle, and j is the site of the white-filled circle. Note that unlike the singlet, the triplet is not symmetric under exchange of i and j: $\frac{1}{\sqrt{2}}\left(a^\dagger_{i\uparrow}a^\dagger_{j\downarrow} + a^\dagger_{i\downarrow}a^\dagger_{j\uparrow}\right) = -\frac{1}{\sqrt{2}}\left(a^\dagger_{j\uparrow}a^\dagger_{i\downarrow} + a^\dagger_{j\downarrow}a^\dagger_{i\uparrow}\right)$

Projected onto the basis $\left\{|1\rangle_{trip}, |2\rangle_{trip}, |3\rangle_{trip}\right\}$, H_{eff} (with $t_d \simeq 0$) becomes:

$$H_{trip} = \begin{pmatrix} \Delta & \sqrt{2}\,(t_{da} - t_a) & -2\sqrt{2}g \\ \sqrt{2}\,(t_{da} - t_a) & \Delta & 0 \\ -2\sqrt{2}g & 0 & 0 \end{pmatrix} \qquad (9)$$

and the ground state of this Hamiltonian is the s-wave triplet state. It should also be noted that the s-wave triplet state is the first excited state of H_{eff} in the limit of large positive Δ.

III. FOUR ATOMS PER PLAQUETTE: THREE $\uparrow$, ONE $\downarrow$

The plaquette occupied by three $\uparrow$ and one $\downarrow$ atoms has only one type of ground state over the full range of Δ. The ground state has s-wave symmetry (i.e. it is unchanged under 90° rotations in the plane of the lattice). The ground state energy is plotted in FIG. 6(a), and the energy difference between the ground state and the first excited state is shown in FIG. 6(b). For this figure the other parameters were $t_{da} = 1.5|g|$ and $t_a = -0.2|g|$.

The ground state can be represented compactly in the pictorial representation introduced above. Here we add an additional symbol to represent a single atom in the $\uparrow$ state. Because the order of the fermionic creation operators matters, we use $\uparrow$ to represent the left creation operator and $\Uparrow$ to represent the right creation

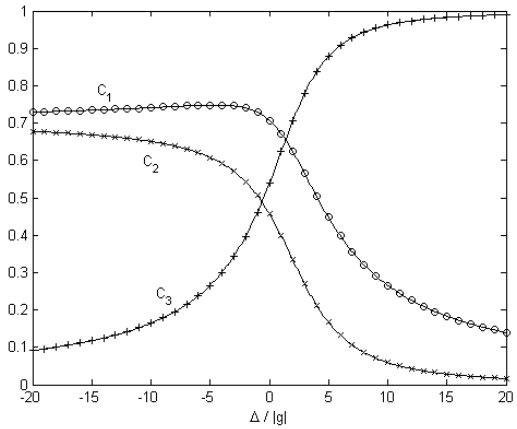

FIG. 7: Components of the ground state (C_1: ∘, C_2: x, C_3: +) vs. Δ for a plaquette occupied by three ↑ and one ↓ atoms. ($t_{da} = 1.5|g|$, $t_a = -0.2|g|$, $t_d = 0$) The marked datapoints were computed from the full Hamiltonian H_{eff}, whereas the solid lines were computed from the projected Hamiltonian $H_{\mathcal{S}}$.

operator. For instance, $\overset{\text{ⓜ}}{\uparrow}\ \overset{\circ}{\Uparrow} = d_1^\dagger a_{3\uparrow}^\dagger a_{4\uparrow}^\dagger |0\rangle$, whereas $\overset{\text{ⓜ}}{\Uparrow}\ \overset{\circ}{\uparrow} = d_1^\dagger a_{4\uparrow}^\dagger a_{3\uparrow}^\dagger |0\rangle$.

The ground state is: $|\psi\rangle_{\mathcal{S}} = C_1 |1\rangle_{\mathcal{S}} + C_2 |2\rangle_{\mathcal{S}} + C_3 |3\rangle_{\mathcal{S}}$, where

$$|1\rangle_{\mathcal{S}} = \frac{1}{2\sqrt{2}} \left(\begin{matrix}\text{ⓜ}\uparrow\\ \circ\Uparrow\end{matrix} + \begin{matrix}\circ\text{ⓜ}\\ \Uparrow\uparrow\end{matrix} + \begin{matrix}\Uparrow\circ\\ \uparrow\text{ⓜ}\end{matrix} + \begin{matrix}\uparrow\Uparrow\\ \text{ⓜ}\circ\end{matrix} + \begin{matrix}\circ\uparrow\\ \text{ⓜ}\Uparrow\end{matrix} + \begin{matrix}\text{ⓜ}\circ\\ \Uparrow\uparrow\end{matrix} + \begin{matrix}\Uparrow\text{ⓜ}\\ \uparrow\circ\end{matrix} + \begin{matrix}\uparrow\Uparrow\\ \circ\text{ⓜ}\end{matrix} \right)$$

$$|2\rangle_{\mathcal{S}} = \frac{1}{2} \left(\begin{matrix}\text{ⓜ}\uparrow\\ \Uparrow\circ\end{matrix} + \begin{matrix}\Uparrow\text{ⓜ}\\ \circ\uparrow\end{matrix} + \begin{matrix}\circ\Uparrow\\ \uparrow\text{ⓜ}\end{matrix} + \begin{matrix}\uparrow\circ\\ \text{ⓜ}\Uparrow\end{matrix} \right)$$

$$|3\rangle_{\mathcal{S}} = \frac{1}{2\sqrt{2}} \left(\begin{matrix}\bullet\uparrow\\ \bullet\Uparrow\end{matrix} + \begin{matrix}\bullet\!-\!\bullet\\ \Uparrow\uparrow\end{matrix} + \begin{matrix}\Uparrow\bullet\\ \uparrow\bullet\end{matrix} + \begin{matrix}\uparrow\Uparrow\\ \bullet\!-\!\bullet\end{matrix} \right)$$

The values of the coefficients C_1, C_2, C_3 are shown in FIG. 7.

Projected onto the three-dimensional subspace of the full Hilbert space with basis vectors $|1\rangle_{\mathcal{S}}$, $|2\rangle_{\mathcal{S}}$, $|3\rangle_{\mathcal{S}}$, H_{eff} (for $t_d \simeq 0$) is:

$$H_{\mathcal{S}} = \begin{pmatrix} \Delta & \sqrt{2}\,(t_a - t_{da}) & -2\sqrt{2}g \\ \sqrt{2}\,(t_a - t_{da}) & \Delta & 0 \\ -2\sqrt{2}g & 0 & 0 \end{pmatrix} \qquad (10)$$

Thus, the ground state of this Hamiltonian is the ground state of H_{eff}. (See solid lines in FIG. 7.)

It should also be noted that the s-wave ground state for 3 ↑, 1 ↓ atoms per plaquette is degenerate with the triplet state for 2 ↑ and 2 ↓ atoms described in the previous section. In fact, the 2 ↑, 2 ↓ triplet state is identical to the ground state for 3 ↑ and 1 ↓ atoms and for 1 ↑ and 3 ↓ atoms, except that the triplet $\frac{1}{\sqrt{2}}\left(a_{i\uparrow}^\dagger a_{j\downarrow}^\dagger + a_{i\downarrow}^\dagger a_{j\uparrow}^\dagger\right)$ is replaced with $a_{i\uparrow}^\dagger a_{j\uparrow}^\dagger$ in the 3 ↑, 1 ↓ case, and with $a_{i\downarrow}^\dagger a_{j\downarrow}^\dagger$ in the 1 ↑, 3 ↓ case.

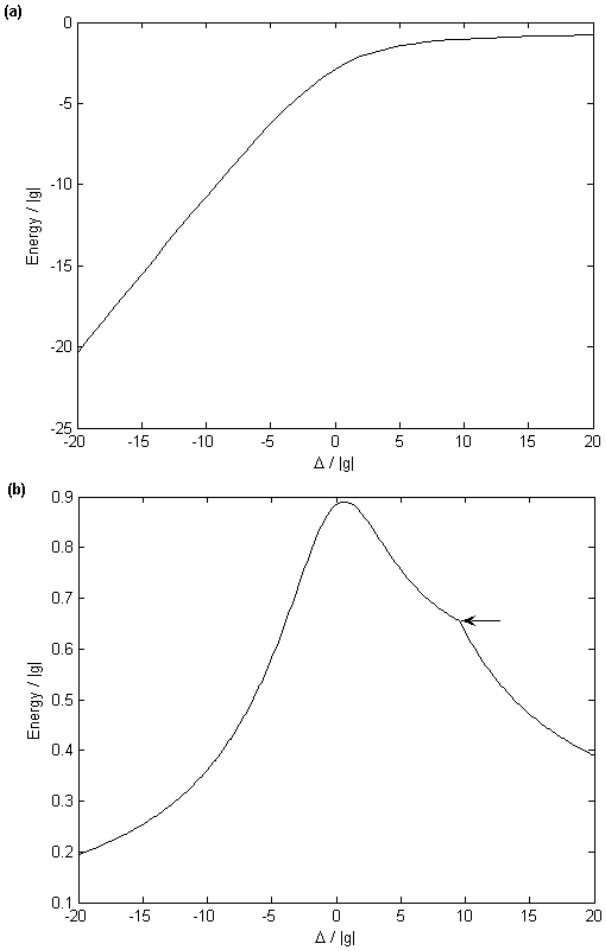

FIG. 8: Energy vs. Δ for a plaquette occupied by one ↑ and one ↓ atom. ($t_{da} = 1.5|g|$, $t_a = -0.2|g|$, $t_d = 0$.) (a): Ground state energy (b): Energy difference between ground state and first excited state. The curve is smooth except at a crossover in the first excited state (indicated by an arrow).

IV. TWO ATOMS PER PLAQUETTE: ONE ↑, ONE ↓

When occupied by only a single atom of each spin state, the plaquette has a single type of ground state for all values of Δ (for values of the other parameters within the typical range). This state is symmetric under 90° rotations – i.e., it has s-wave symmetry. The ground state energy of this system is plotted in figure 8(a). Figure 8(b) shows the excitation gap between the ground state and first excited state. Both these figures assume typical values of t_{da} and t_a ($t_{da} = 1.5|g|$, $t_a = -0.2|g|$).

The ground state can be expressed as a vector in a 3-dimensional subspace of the full Hilbert space. The basis vectors of this subspace (in the pictorial representation

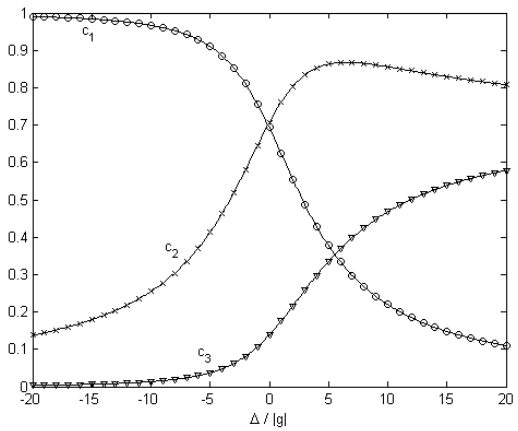

FIG. 9: Components of the ground state (c_1: ∘, c_2: x, c_3: ▽) vs. Δ for a plaquette occupied by one ↑ and one ↓ atom. ($t_{da} = 1.5|g|$, $t_a = -0.2|g|$, $t_d = 0$) The marked datapoints were computed from the full Hamiltonian H_{eff}, whereas the solid lines were computed from the projected Hamiltonian H.

introduced above) are:

$|1\rangle = \frac{1}{2}$ (ⓜ ∘ / ∘ ∘ + ∘ ⓜ / ∘ ∘ + ∘ ∘ / ∘ ⓜ + ∘ ∘ / ⓜ ∘)

$|2\rangle = \frac{1}{2}$ (▬ / ∘ ∘ + ∘ ∘ / ▮ ∘ + ∘ ∘ / ∘ ▬ + ▮ ∘ / ∘ ∘)

$|3\rangle = \frac{1}{\sqrt{2}}$ (∘ ∘ / ∘ ∘ + ∘ ∘ / ∘ ∘)

Thus, the ground state is given by: $|\psi\rangle = c_1|1\rangle + c_2|2\rangle + c_3|3\rangle$, where the values of the coefficients c_1, c_2, c_3 are shown in FIG. 9

Projected onto this subspace, H_{eff} (for $t_d \simeq 0$) expressed in the above basis becomes:

$$H = \begin{pmatrix} \Delta & -2\sqrt{2}g & 0 \\ -2\sqrt{2}g & 0 & 2\sqrt{2}t_a \\ 0 & 2\sqrt{2}t_a & 0 \end{pmatrix} \qquad (11)$$

Thus, the ground state of this Hamiltonian is the ground state of H_{eff}. (See solid lines on FIG. 9.)

V. THREE ATOMS PER PLAQUETTE:TWO ↑, ONE ↓

The plaquette with two ↑ atoms and one ↓ atom has three distinct types of ground states for different values of the parameter Δ (with the other parameters in the typical range). However, over a wide range of Δ around $\Delta = 0$ the system is in the same type of ground state. The ground state of this type is two-fold degenerate. (Hence, we will refer to this as the "degenerate state".) The ground state energy and the gap between the ground state and first excited state are shown in FIG. 10. (For the full range of Δ values shown in the figure, the system is in the degenerate state.) The degenerate ground states (which we call $|\psi\rangle_+$ and $|\psi\rangle_-$) can be defined in such a way that they are eigenstates of a 90° rotation in the plane of the plaquette, in which case $|\psi\rangle_\pm$ gains a factor of $\pm i$ under such a rotation.

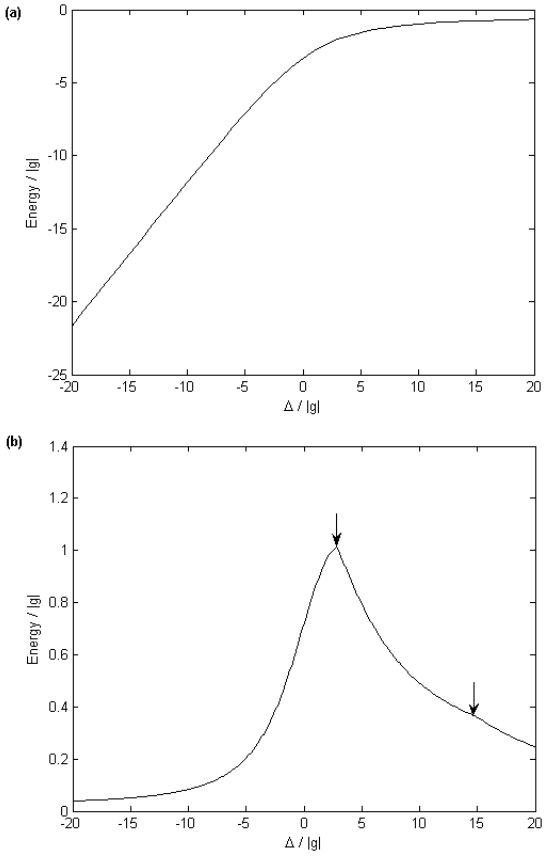

FIG. 10: Energy vs. Δ for a plaquette occupied by two ↑ and one ↓ atoms. ($t_{da} = 1.5|g|$, $t_a = -0.2|g|$, $t_d = 0$) (a): Ground state energy (b): Energy difference between ground state and first excited state. Crossovers in the first excited state (at which points the curve is not smooth) are indicated by arrows.

The state $|\psi\rangle_+$ can be expressed as a vector in a particular six-dimensional subspace of the full Hilbert space. We define the basis vectors of this subspace in the pictorial representation introduced above. However, because the order of the fermionic creation operators matters, we use three symbols ↑, ⇑, ∧ (↓, ⇓, ∨) to represent the first, second, and third creation operator for atoms in the ↑ (↓) state. E.g., ∧ ∘ / ⇓ ↑ $= a^\dagger_{4\uparrow}a^\dagger_{3\downarrow}a^\dagger_{1\uparrow}|0\rangle$. Represented in this way, the six basis vectors are:

$|1\rangle_+ = \frac{1}{2}\big[$(ⓜ ↑ / ∘ ∘ − ∘ ∘ / ↑ ⓜ)$-i$(∘ ⓜ / ∘ ↑ − ↑ ∘ / ⓜ ∘)$\big]$

$|2\rangle_+ = \frac{1}{2}\big[$(↑ ⓜ / ∘ ∘ − ∘ ∘ / ⓜ ↑)$-i$(∘ ↑ / ∘ ⓜ − ⓜ ∘ / ↑ ∘)$\big]$

$|3\rangle_+ = \frac{1}{2}\big[$(ⓜ ∘ / ∘ ↑ − ↑ ∘ / ∘ ⓜ)$-i$(∘ ⓜ / ↑ ∘ − ∘ ↑ / ⓜ ∘)$\big]$

$|4\rangle_+ = \frac{1}{2}\big[$(↑ ⇓ / ∘ ∧ − ∧ ∘ / ⇓ ↑)$-i$(∘ ↑ / ∧ ⇓ − ⇓ ∧ / ↑ ∘)$\big]$

$$|5\rangle_+ = \tfrac{1}{2}\Big[\Big(\downarrow\ \Uparrow\ -\wedge\ \circ\ \Big) - i\Big(\circ\ \downarrow\ -\Uparrow\ \wedge\ \Big)\Big]$$
$$|6\rangle_+ = \tfrac{1}{2}\Big[\Big(\Uparrow\ \vee\ -\circ\ \uparrow\ \Big) - i\Big(\uparrow\ \Uparrow\ -\vee\ \circ\ \Big)\Big]$$

and the state $|\psi\rangle_+$ is given by:

$$|\psi\rangle_+ = A\,|1\rangle_+ + A^*\,|2\rangle_+ + B\,|3\rangle_+ + C\,|4\rangle_+ + D\,|5\rangle_+ + D^*\,|6\rangle_+ \quad (12)$$

for some complex coefficients A, B, C, and D. Note that under a 90° clockwise rotation $|n\rangle_+ \to i\,|n\rangle_+$ for each n, and thus $|\psi\rangle_+ \to i\,|\psi\rangle_+$. The state $|\psi\rangle_-$ can be expressed as a vector in a six-dimensional subspace of the full Hilbert space with basis vectors

$$|n\rangle_- = |n\rangle_+^* \quad (13)$$

for $n = 1, ..., 6$. $|\psi\rangle_-$ is given by:

$$|\psi\rangle_- = A^*\,|1\rangle_- + A\,|2\rangle_- + B^*\,|3\rangle_- + C^*\,|4\rangle_- + D^*\,|5\rangle_- + D\,|6\rangle_- = |\psi\rangle_+^* \quad (14)$$

The complex coefficients A, B, C, and D can be written as:

$$A = |A|\,e^{i\phi_A},\ D = |D|\,e^{i\phi_D}$$
$$B = |B|\,e^{i\pi/4},\ C = |C|\,e^{i\pi/4} \quad (15)$$

where $|A|$, $|B|$, $|C|$, $|D|$, ϕ_A, and ϕ_D depend on the parameters of H_{eff}. The coefficients are determined up to an arbitrary overall phase, which here was chosen to fix the phases of B and C as shown. (B and C were found to have the same phase.) For typical values of $t_a = -0.2|g|$, $t_{da} = 1.5|g|$, $t_d = 0$, the values of these parameters (vs. Δ) are shown in FIG. 11.

Projected onto the subspace with basis $\{|1\rangle_+, |2\rangle_+, |3\rangle_+, |4\rangle_+, |5\rangle_+, |6\rangle_+\}$, H_{eff} (expressed in that basis) is (for $t_d \simeq 0$):

$$H_+ = \begin{pmatrix} \Delta & t_{da} & t_a & -ig & ig & 0 \\ t_{da} & \Delta & -it_a & g & 0 & ig \\ t_a & it_a & \Delta & -2g & g & -ig \\ ig & g & -2g & 0 & -it_a & t_a \\ -ig & 0 & g & it_a & 0 & -t_a \\ 0 & -ig & ig & t_a & -t_a & 0 \end{pmatrix} \quad (16)$$

The ground state of H_+ is thus $|\psi\rangle_+$. (See solid lines in FIG. 11.) Projected onto the subspace with basis $\{|1\rangle_-, |2\rangle_-, |3\rangle_-, |4\rangle_-, |5\rangle_-, |6\rangle_-\}$, H_{eff} is given by:

$$H_- = H_+^* = H_+^T \quad (17)$$

(Note that in this equation H_+ is still expressed in the basis in which it was defined above.) Thus the ground state of H_- is $|\psi\rangle_+^* = |\psi\rangle_-$.

For Δ far to the negative side ($\Delta < -92.9\,|g|$ for $t_{da} = 1.5|g|$, $t_a = -0.2|g|$, $t_d = 0$), the system of two

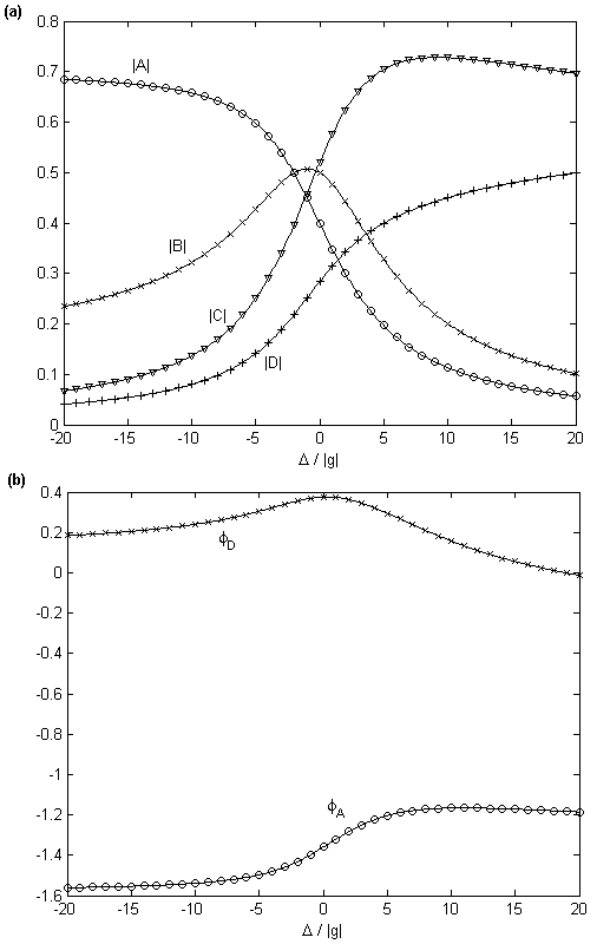

FIG. 11: Ground state parameters vs. Δ for a plaquette occupied by two $\uparrow$ and one $\downarrow$ atoms. ($t_{da} = 1.5|g|$, $t_a = -0.2|g|$, $t_d = 0$) (a): Amplitudes ($|A|$: $\circ$, $|B|$: x, $|C|$: $\triangledown$, $|D|$: +). (b): Phases (ϕ_A: $\circ$, ϕ_D: x). The overall phase was chosen to give $B = |B|\,e^{i\pi/4}$ and $C = |C|\,e^{i\pi/4}$. The marked datapoints on (a) and (b) were computed from the full Hamiltonian H_{eff}, whereas the solid lines were computed from the projected Hamiltonian H_+.

$\uparrow$ atoms and one $\downarrow$ atom on a plaquette has a non-degenerate d-wave ground state. This state can be expressed as a vector in a 3-dimensional subspace of the full Hilbert space of this system, with basis vectors:

$$|1\rangle_{left} = \tfrac{1}{2\sqrt{2}}\Big(\begin{matrix}\text{ⓜ}\uparrow\\ \circ\ \circ\end{matrix} - \begin{matrix}\circ\ \text{ⓜ}\\ \circ\ \uparrow\end{matrix} + \begin{matrix}\circ\ \circ\\ \uparrow\ \text{ⓜ}\end{matrix} - \begin{matrix}\uparrow\ \circ\\ \text{ⓜ}\ \circ\end{matrix} - \begin{matrix}\uparrow\ \text{ⓜ}\\ \circ\ \circ\end{matrix} + \begin{matrix}\circ\ \uparrow\\ \circ\ \text{ⓜ}\end{matrix} - \begin{matrix}\circ\ \circ\\ \text{ⓜ}\ \uparrow\end{matrix} + \begin{matrix}\text{ⓜ}\ \circ\\ \uparrow\ \circ\end{matrix}\Big)$$

$$|2\rangle_{left} = \tfrac{1}{2}\Big(-\begin{matrix}\text{ⓜ}\ \circ\\ \circ\ \uparrow\end{matrix} + \begin{matrix}\circ\ \text{ⓜ}\\ \uparrow\ \circ\end{matrix} - \begin{matrix}\uparrow\ \circ\\ \circ\ \text{ⓜ}\end{matrix} + \begin{matrix}\circ\ \uparrow\\ \text{ⓜ}\ \circ\end{matrix}\Big)$$

$|3\rangle_{left} = \frac{1}{2}\Big($  $\Big)$

$= \frac{1}{2}\Big($ 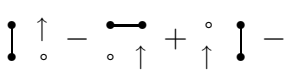 $\Big)$

Note that there is some ambiguity in which spins to group into a singlet and which to write as $\uparrow$, as evidenced by the two forms given for $|3\rangle_{left}$ (the first of which has the advantage of all its terms being orthogonal, but the second of which makes more obvious how the Hamiltonian connects it to components $|1\rangle_{left}$ and $|2\rangle_{left}$).

H_{eff} (for $t_d \simeq 0$) projected onto this subspace expressed in the basis $\left\{|1\rangle_{left}, |2\rangle_{left}, |3\rangle_{left}\right\}$ is:

$$H_{left} = \begin{pmatrix} \Delta - t_{da} & -\sqrt{2}t_a & -g \\ -\sqrt{2}t_a & \Delta & -\sqrt{2}g \\ -g & -\sqrt{2}g & t_a \end{pmatrix} \qquad (18)$$

Thus, the ground state of this Hamiltonian is the ground state of H_{eff} in the left-most region ($\Delta < -92.9\,|g|$).

For Δ far to the positive side ($\Delta > 97.9\,|g|$ for $t_{da} = 1.5|g|$, $t_a = -0.2|g|$, $t_d = 0$), the system has a non-degenerate s-wave ground state. Furthermore, in this state the ground state wavefunction and energy are constant for changing Δ. In the pictorial representation this ground state is given by:

$|\psi\rangle_{right} = \frac{1}{2\sqrt{6}}\Big($ 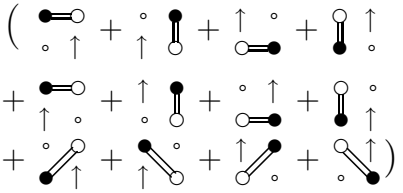 $\Big)$

The energy of this state is $H_{right} = 2t_a$.

It should be noted that the case of 1 $\uparrow$, 2 $\downarrow$ atoms on a plaquette is equivalent to the 2 $\uparrow$, 1 $\downarrow$ case under exchange of $\uparrow$ and $\downarrow$ spins. The Hamiltonian H_{eff} is invariant under such a spin exchange, except for a change in the sign of g. This is equivalent to replacing $d^\dagger$ with $-d^\dagger$. Thus, the eigenenergies of these two cases are identical, and the eigenstates are identical except for a change in the sign of the components which include a dressed molecule.

VI. SUMMARY AND DISCUSSION

In the above, we have investigated the ground state properties of the system with different numbers of spin $\uparrow$ and $\downarrow$ atoms occupying the four-site plaquette in an optical superlattice. All the other cases can be reduced to one of the configurations considered above, or to a trivial case, through the particle-hole exchange. (Cases where all particles are in the same spin state are non-interacting, and thus trivial.) For instance, for five atoms with three spin-$\downarrow$ and two spin-$\uparrow$, one has two spin-$\uparrow$ and one spin-$\downarrow$ holes in that plaquette. So, the states are equivalent to those in the case with two spin-$\uparrow$ and one spin-$\downarrow$ atoms, but with exchange of the parameters t_{da} and t_a in the effective Hamiltonian H_{eff}. The sign of g also changes, but as noted above this is equivalent to replacing $d^\dagger$ with $-d^\dagger$. Thus this change has no effect on the eigenenergies, and the eigenstates only experience a change in the sign of those components where the plaquette is occupied by an odd number of dressed molecules. In addition, if particle-hole exchange changes the number of atoms by N, then the eigenenergies are shifted by $\frac{N}{2}\Delta$.

From this investigation, we have seen that even on a single plaquette, the Hamiltonian H_{eff} exhibits a number of different types of ground state configurations, possessing various forms of rotational symmetry (s-wave, d-wave, etc.). There are level crossings between these different types of ground states as the detuning Δ is varied. The change of the ground state symmetry from s-wave to d-wave as one scans the parameter Δ from negative to positive regions may be a general feature and not limited to a single plaquette. For a large lattice, this symmetry change might correspond to a quantum phase transition from the s-wave to the d-wave superfluidities [19]. The states found in this work on a single plaquette also provide some basic entries for constructing the effective many-body Hamiltonian for atoms in a quasi-two-dimensional optical lattice through the contractor renormalization method [13, 14]. When the average filling number of the lattice is close to a half with hole doping, one expects that the basic degrees of freedom from each plaquette are the ground state configurations specified in Sec. II, the fermionic hole excitations given by the states in Sec. V, the bosonic hole-pair excitations specified in Sec. IV, and the bosonic spin excitations given by the states in Sec. III and II. The effective many-body Hamiltonian will then describe the interaction between these basic degrees of freedom. So, it is our hope that the investigation of the single-plaquette physics here will make it possible to better understand the physics of strongly interacting fermions on larger lattices.

This work was supported by the NSF awards (0431476), the ARDA under ARO contracts, and the A. P. Sloan Fellowship.

[1] C.A. Regal, M. Greiner and D.S. Jin, Phys. Rev. Lett. 92, 040403 (2004); M.W. Zwierlein et al., Phys. Rev. Lett. 92, 120403 (2004); C. Chin et al., Science 305, 1128 (2004).

[2] M. Greiner, et al., Nature 415, 39 (2002); C. Orzel, et al., Science 291, 2386 (2001); D. Jaksch, et al., Phys. Rev. Lett. 81, 3108 (1998).

[3] For a review, see D. Jaksch and P. Zoller, Annals of Physics 315, 52 (2005).

[4] For a review, see R.A. Duine and H.T.C. Stoof, Phys. Rep. 396, 115 (2004); Q. Chen et al., Phys. Reports 412, 1 (2005).
[5] D. B. M. Dickerscheid et al., Phys. Rev. A 71, 043604 (2005); Phys. Rev. Lett. 94, 230404 (2005).
[6] L.-M. Duan, Phys. Rev. Lett. 95, 243202 (2005).
[7] L. Carr and M. Holland, Phys. Rev. A 72, 031604 (2005); F. Zhou, Phys. Rev. B 72, 220501 (R)(2005); F. Zhou and C. Wu, cond-mat/0511589.
[8] R. B. Diener and T.-L. Ho, Phys. Rev. Lett. 96, 010402 (2006); Phys. Rev. A 73, 017601 (2006).
[9] M. Kohl et al., Phys. Rev. Lett. 94, 080403 (2005); T. Stoeferle et al., Phys. Rev. Lett. 96, 030401 (2006).
[10] K. Xu et al., cond-mat/0507288.
[11] S. R. White and D. J. Scalapino, Phys. Rev. B 55, 06504 (1997).
[12] L.-M. Duan, E. Demler, M. D. Lukin, Phys. Rev. Lett. 91, 090402 (2003).
[13] C. J. Morningstar and M. Weinstein, Phys. Rev. D 54 4131 (1996).
[14] E. Altman, A. Auerbach, Phys. Rev. B 65, 104508 (2002).
[15] J. Sebby-Strabley, M. Anderlini, P. S. Jessen, J. V. Porto, cond-mat/0602103 and refs therein.
[16] S. Trebst, U. Schollwoeck, M. Troyer, P. Zoller, cond-mat/0506809.
[17] W. Hofstetter et al., Phys. Rev. Lett. 89, 220407 (2002).
[18] P. W. Anderson, Science 235, 1196 (1987).
[19] For a review, see R. Micnas, J. Ranninger, and S. Robaszkiewicz, Rev. Mod. Phys. 62, 113 (1990).